Lattice dynamics of $BaTiO_3$ in the cubic phase

1989 J. Phys.: Condens. Matter 1 9811

(http://iopscience.iop.org/0953-8984/1/49/002)

J. Phys.: Condens. Matter **1** (1989) 9811–9822. Printed in the UK

Lattice dynamics of $BaTiO_3$ in the cubic phase

D Khatib†, R Migoni‡, G E Kugel§ and L Godefroy†

† Laboratoire de Physique du Solide (UA 785), Université de Bourgogne, BP 138, 21004 Dijon, France

‡ IFIR, Av. Pellegrini 250, 2000 Rosario, Argentina

§ CLOES-SUPELEC-Technopole de Metz, 2 rue Edouard Belin, F 57078 Metz Cédex, France

Received 6 April 1988, in final form 31 May 1989

Abstract. We have calculated the phonon dispersion curves of baryum titanate ($BaTiO_3$) in the cubic phase. A non-linear shell model is used, in which the fourth-order anharmonic core–shell interaction of the oxygen ion is considered within a self-consistent phonon approximation. The temperature dependence of the ferroelectric soft mode is reproduced by our calculations, leading to the linear and non-linear contributions of the oxygen polarisability. The values of the relevant model parameters are critically analysed.

1. Introduction

$BaTiO_3$ is the first ferroelectric material to be discovered (Shirane and Hoshino 1951) that undergoes successive structural phase transitions on cooling of cubic (C) to tetragonal (T) to orthorhombic (O) to rhombohedral (R) (Lines and Glass 1977). The soft-mode concept was introduced by Cochran (1960) for the ferroelectricity that occurs in this compound, and, since then, many other cases of soft modes have been studied both experimentally and theoretically (Bruce and Cowley 1981, Müller and Thomas 1981). Underdamped soft modes, leading to a structural phase transition of a displacive nature have been reported in $SiTiO_3$, $KTaO_3$ (Fleury and Worlock 1968, Shirane *et al* 1967) and in $KTa_{1-x}Nb_xO_3$ (KTN) (Kugel *et al* 1987). In these systems, the anharmonicity is small and the ferroelectric mode does not freeze out, or else freezes out at very low temperatures.

In $BaTiO_3$, as in $KNbO_3$, the soft mode is highly overdamped (Spitzer *et al* 1962, Barker and Hopfield 1964, Harada *et al* 1971, Inoue and Asai 1981). It becomes overdamped below about 1200 K (Luspin *et al* 1980) and the damping diverges when approaching T_c (Vogt *et al* 1982). Here the debate as to whether the phase transition is more displacive or order–disorder-like is still active. Infrared experiments (Luspin *et al* 1980) indicate a stabilisation in energy of the ferroelectric soft mode at about 80 cm^{-1}, with temperature decreasing towards T_c. This, as well as deviation of the static dielectric constant from the behaviour predicted from the lattice modes, has been interpreted as being caused by additional relaxation related to dynamical disorder (Müller *et al.* 1982). In the same temperature range above T_c Burns and Dacol (1982) also observed deviations from linearity of the optic refraction index against temperature that are consistent with

0953-8984/89/469811 + 12 $02.50

the appearance of polarisation. On the other hand, hyper-Raman measurements can be interpreted in terms of one heavily overdamped oscillator only, which continues to soften toward the transition (Vogt *et al* 1982, Presting *et al* 1983). However, recent EPR experiments (Müller and Berlinger 1986) confirm a relaxator behaviour and are in favour in $BaTiO_3$, as in $KNbO_3$ (Fontana and Kugel 1985), of a crossover phenomenon from displacive to order–disorder mechanism with decreasing temperature.

Considering these basic aspects, it is rather questionable to try explaining the phase transitions in $BaTiO_3$ using dynamical lattice models, even if strong anharmonic contributions are taken into account. Nevertheless, in this paper, the dynamical properties of $BaTiO_3$ in the cubic phase are re-examined in the framework of a strongly anharmonic lattice model. The aim of our calculation is less to explain the behaviour of the system at the transition than to point out the interactions leading to loss of strong stability and eventually enabling crossover to a different behaviour on approaching T_c. This approach can be justified by several arguments, by considering, for example, the following questions. What are the main interactions linking the whole lattice in $BaTiO_3$? How far do the parameters involved differ from those of parent compounds such as $SrTiO_3$ and even $KTa_{1-x}Nb_xO_3$? Since the displacive nature plays a major role far from the structural phase transition, which anharmonicity is able to explain the mode softening?

The purpose of the present paper is to shed light on such questions. This is done by applying to $BaTiO_3$ a dynamical shell model in which an anharmonic coupling localised on the oxygen site is introduced. The main objective of our paper is to emphasise the likely importance of this particular anharmonic coupling and in the work described here all other anharmonicities have been neglected. There is, as discussed further in § 2, reason to believe that in a full analysis of anharmonic effects in $BaTiO_3$, other anharmonic terms (specifically cubic terms) will prove to be significant. Thus the significance attached to our quantitative conclusions on anharmonic behaviour should be restricted to the evidence they provide for the nature and possible importance of contributions from quartic anharmonicity associated with the polarisability of the oxygen ion. Two series of model parameters are obtained in order to analyse the experimental phonon dispersion curves measured by Harada *et al* (1971) and by Jannot *et al* (1981). The influence of temperature on some critical dispersion branches is studied in detail.

2. Model description

Various microscopic models in which the anharmonic contributions to the self-energy renormalise the phonon frequencies of the lattice modes have been employed (Bruce and Cowley 1981). In our case, we consider a model introduced by Migoni *et al* (1976) including, as the anharmonic part, a quartic on-site ion-shell interaction in the oxygen ion. This assumption takes into account the anisotropic and non-linear polarisability of the O^{2-} ion. Such anharmonic interaction alone explains the relevant phonon shifts in $SrTiO_3$ (Migoni *et al* 1976), $KTaO_3$ (Migoni *et al* 1977) and KTN (Kugel *et al* 1987). It is interesting to investigate the consequences of restricting attention to this interaction also for $BaTiO_3$, in particular since in this case only the lowest TO long-wavelength phonon (the ferroelectric mode) is strongly affected by a change of temperature (Luspin *et al* 1980). In the case of $BaTiO_3$, however, there is substantial broadening of the mode, which must be ascribed to cubic effects neglected in such a treatment. These cubic terms will also affect the temperature dependence of the frequency, so there is clearly some

error involved in ascribing all such temperature dependence to the quartic oxygen coupling, as is done in the present model.

The three-dimensional anharmonic-shell model that is used here is an extension of the harmonic-shell model employed by Cowley (1964) and Stirling (1972) for $SrTiO_3$ and contains a set of 15 model parameters. Figure 1 schematically represents the interactions involved in our case.

The six short-range parameters A_{AO}, B_{AO}, A_{BO}, B_{BO}, A_{OO} and B_{OO} are the axially symmetric force constants A and B between Ba–O, Ti–O and O–O ions respectively. The ionic and shell charges are given by Z_A, Z_O, Y_A, Y_B and Y_O. Z_B is obtained with the neutrality condition. The parameters k_A and k_B are the core–shell force constants for the A(Ba) and B(Ti) ions respectively.

The oxygen core–shell interaction is anisotropic, with harmonic couplings k_2^{O-B} along the O–B chain and k_2^{O-A} perpendicular to it. The only anharmonic interaction included in the model is a non-linear extension of k_2^{O-B}, called k_4^{O-B}, which must be of order four in the shell displacement because of the inversion symmetry at the O site. Both harmonic and anharmonic core–shell couplings at the oxygen are pointed out on figure 1. The

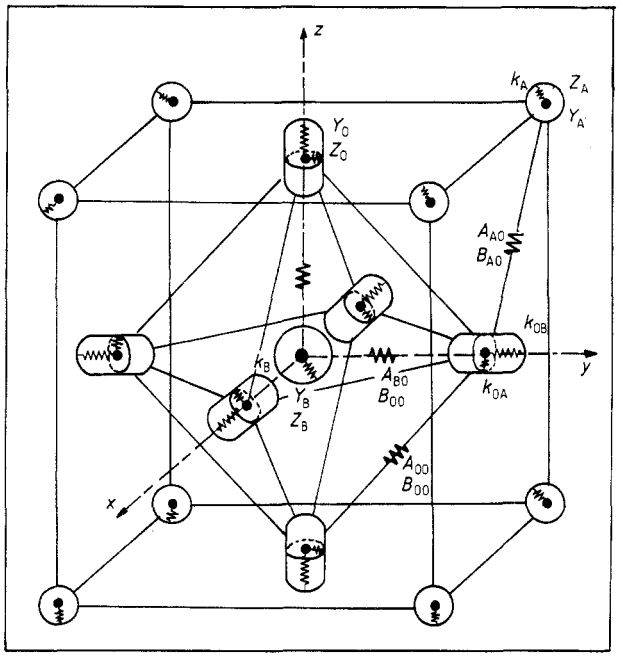

Figure 1. Schematic representation of the lattice-dynamical model and its parameters.

expansion of the oxygen core–shell interaction potential in terms of the relative shell displacements $w(l, O_\alpha)$ is thus assumed to be of the form

$$\varphi_O = \varphi_2^{O-A} + \varphi_2^{O-B} + \varphi_4^{O-B} \tag{1}$$

$$= \tfrac{1}{2}k_2^{O-A} \sum_{\substack{l,\alpha,\beta \\ (\beta\neq\alpha)}} w_\beta^2(l, O_\alpha) + \tfrac{1}{2}k_2^{O-B} \sum_{l,\alpha} w_\alpha^2(l, O_\alpha) + \frac{1}{4!}k_4^{O-B} \sum_{l,\alpha} w_\alpha^4(l, O_\alpha) \tag{2}$$

where α labels the Cartesian components, l is the cell index and O_α indicates the oxygen ion located on the line O–Ti in the α direction. Note that only the oxygen shell displacements along O–Ti chains are assumed to respond to a non-linear interaction.

Within the self-consistent phonon approximation (SPA), the non-linear potential yields a temperature dependent core–shell coupling constant $k_{OB}(T)$ acting along the O–B direction and given by

$$k_{OB}(T) = k_2^{O-B} + \tfrac{1}{2}k_4^{O-B}\langle w_{OB}^2\rangle_T. \tag{3}$$

The quantity $\langle w_{OB}^2\rangle_T$ is the thermal average of the oxygen relative core–shell displacement w toward the B(Ti) ion, and is obtained as

$$\langle w_{OB}^2\rangle_T = \frac{\hbar}{2Nm_O}\sum_{q,j}\frac{f_\alpha^2(O_\alpha|q,j)}{\omega(q,j)}\coth\frac{\hbar\omega(q,j)}{2k_BT} \tag{4}$$

where m_O is the mass of the oxygen ion, N is the number of q points considered in the summation, k_B is the Boltzmann constant and $\omega(q,j)$ is the frequency of the phonon with branch index j and wave vector q. The shell eigenvectors $f(q,j)$ are obtained from the core eigenvectors $e(q,j)$ with the expression (Cochran 1960, Cowley 1964)

$$f(q,j) = \mathbf{M}^{-1/2}(\mathbf{S} + \mathbf{K} + \boldsymbol{\Delta}^{-1}\mathbf{T}^+\mathbf{M}^{-1/2}e(q,j) \tag{5}$$

where $\mathbf{M}$ is the mass matrix, $\mathbf{T}$ and $\mathbf{S}$ are the Fourier transforms of the inter-ionic ion–shell and shell–shell coupling matrices commonly used in the shell–model, including the corresponding Coulomb interactions, and $\mathbf{K}$ is the intra-ionic core–shell coupling matrix. The contribution $\boldsymbol{\Delta}$ added to $\mathbf{K}$ in our case is due to the quartic term in the potential expansion with

$$\Delta_{\alpha\beta}^{\kappa\kappa'} = \tfrac{1}{2}k_4^{O-B}\langle w_{OB}^2\rangle_T\delta_{\alpha\beta}\delta_{\kappa O_\alpha}\delta_{\kappa' O_\beta}. \tag{6}$$

This additional term renormalises the dynamical matrix $\mathbf{D}$ such that

$$\mathbf{D} = \mathbf{M}^{-1/2}[\mathbf{R} - \mathbf{T}(\mathbf{S} + \mathbf{K} + \boldsymbol{\Delta})^{-1}\mathbf{T}^+]\mathbf{M}^{-1/2} \tag{7}$$

where $\mathbf{R}$ is the ion–ion coupling matrix of the shell model. Since in the present case the short-range inter-ionic forces act only between shells, the matrices $\mathbf{R}$, $\mathbf{T}$ and $\mathbf{S}$ differ only in their Coulomb contributions.

3. Results of the calculations

3.1. Quasi-harmonic model parameters and dispersion curves at 421 K

The 15 parameters of our model, including the effective harmonic $k_{OB}(T)$, have been obtained by fitting our theoretical model to the experimental phonon-dispersion curves measured at 421 K by Jannot *et al* (1981) and by Harada *et al* (1971) using neutron spectroscopy.

The parameters k_2^{O-B} and k_4^{O-B} contained in $k_{OB}(T)$ are subsequently determined as explained in § 3.2 by fitting the temperature dependence of the ferroelectric mode as measured by infrared techniques (Luspin *et al* 1980).

Two sets of model parameters interpreting the phonon dispersion curves at 421 K have been calculated. The first result (called model I) originates from a global fitting of the whole set of model parameters to the dispersion curves, all the parameters being free to vary. A second series of parameters (denoted model II) is an improved version.

In this model, the short-range parameters A_{BO}, B_{BO}, A_{OO} and B_{OO} have been determined from the values obtained by Migoni *et al* (1976) on the parent compound $SrTiO_3$ containing the same TiO_6 octahedron by assuming that the ions interact through the repulsive Born–Mayer potential function

$$\varphi_{\kappa\kappa'}(\boldsymbol{r}_{\kappa\kappa'}) = \lambda_{\kappa\kappa'} \exp(-\boldsymbol{r}_{\kappa\kappa'}/\rho_{\kappa\kappa'}) \tag{8}$$

where $\boldsymbol{r}_{\kappa\kappa'}$ is the distance between atoms of type κ and κ' and $\rho_{\kappa\kappa'}$ and $\lambda_{\kappa\kappa'}$ are interaction constants.

Since in the case of $SrTiO_3$ the phonon frequencies are known with great accuracy, the parameters between Ti and O ions can be considered as being highly reliable and are extended to the case of $BaTiO_3$. Since $A_{\kappa\kappa'} = (d^2\varphi_{\kappa\kappa'}/dr^2)_{r=r_{\kappa\kappa'}}$ and $B_{\kappa\kappa'} = (r^{-1}d\varphi_{\kappa\kappa'}/dr)_{r=r_{\kappa\kappa'}}$, it follows from (8) that the relations between the force constants $A_{\kappa\kappa'}$, $B_{\kappa\kappa'}$ corresponding to an interatomic distance r in a given compound, and $A'_{\kappa\kappa'}$, $B'_{\kappa\kappa'}$ for a different r' in a parent compound are

$$A' = A \exp[(A/B)(r' - r)/r] \qquad B' = B(r/r') \exp[(A/B)(r' - r)/r] \tag{9}$$

where the subindices $\kappa\kappa'$ are dropped everywhere for the sake of simplicity.

Table 1. Shell-model parameters of $BaTiO_3$ obtained for both model I and II and comparison with the corresponding parameters of $SrTiO_3$, $KTaO_3$ and $KNbO_3$. The values of the k_2^{O-B} and k_4^{O-B} have been calculated within the self-consistent procedure with the model II in $BaTiO_3$. Since the parameter values of model I are only slightly different (especially for k_{OB}) similar values of k_2^{O-B} and k_4^{O-B} are expected for model I.

	A_{OA}	B_{OA}	A_{OB}	B_{OB} ($e^2/2v$)	A_{OO}	B_{OO}	Z_A	Z_O (e)
$BaTiO_3$ Model I	33.20	−4.96	270.5	−41.57	2.80	1.15	1.67	−1.64
Model II	34.95	−4.60	258.3	−37.66	2.21	0.84	1.86	−1.68
$SrTiO_3$	26.0	−4.25	285.0	−43.0	1.90	0.74	1.62	−1.64
$KTaO_3$, $KNbO_3$	14.65	−1.01	359.0	−68.0	3.22	1.08	0.82	−1.88

	Y_A	Y_B (e)	Y_O	k_A	k_B	k_{OA} (e^2/v)	k_{OB} (421 K)	k_2^{O-B} (e^2/v)	k_4^{O-B} (e^2 Å$^{-2}/v$)
$BaTiO_3$ Model I	−5.00	−1.54	−2.63	1620	1415	600.3	102.9	—	—
Model II	−3.76	−1.58	−2.59	1119	1429	450.1	92.5	137.0	−9000
$SrTiO_3$	2.30	−1.50	−2.70	57	1446	626.0	103.4	98.6	1960
$KTaO_3$	−0.42	7.83	−3.01	1000	1283	410.0	360.2	341.8	23400
$KNbO_3$							—	269.0	57000

The parameters obtained for both fits are reported in table 1 and are compared to the corresponding values determined on $SrTiO_3$ (Migoni *et al* 1976), $KTaO_3$ (Migoni *et al* 1977) and $KNbO_3$ (Kugel *et al* 1987). The dispersion curves are represented on figures 2 (model I) and 3 (model II) together with the experimental points. On figure 3, the dispersion curves calculated by Jannot *et al* (1981) are added for comparison.

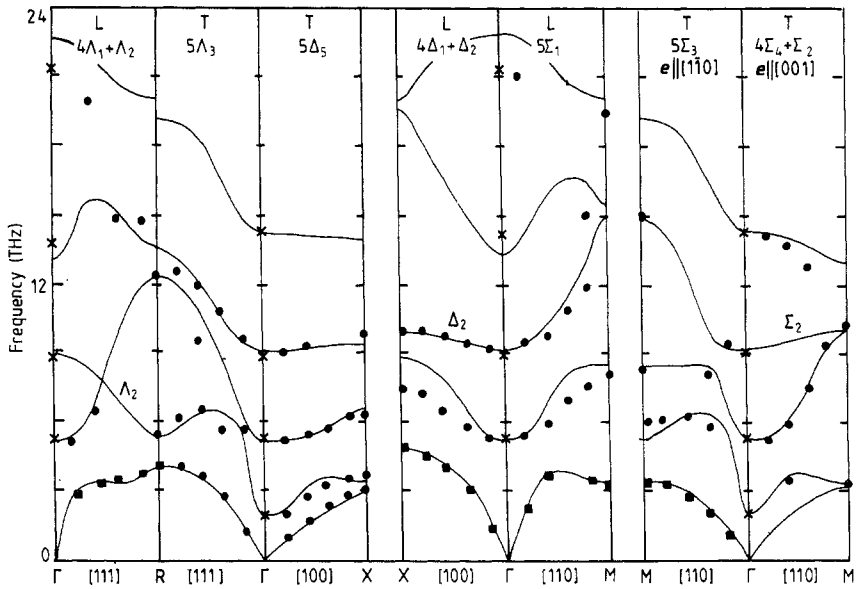

Figure 2. Phonon-dispersion curves calculated in $BaTiO_3$ at 421 K with model I and compared with experimental data obtained by neutron scattering (full circles: Jannot *et al* 1981; full squares: Harada *et al* 1971) and by infrared spectroscopy (crosses: Luspin *et al* 1980).

The agreement between theory and experiment is revealed to be better than for previous calculations (Jannot *et al* 1981), especially for model II. This is particularly true for the high-frequency branches above 10 THz, and also for the two lowest-frequency

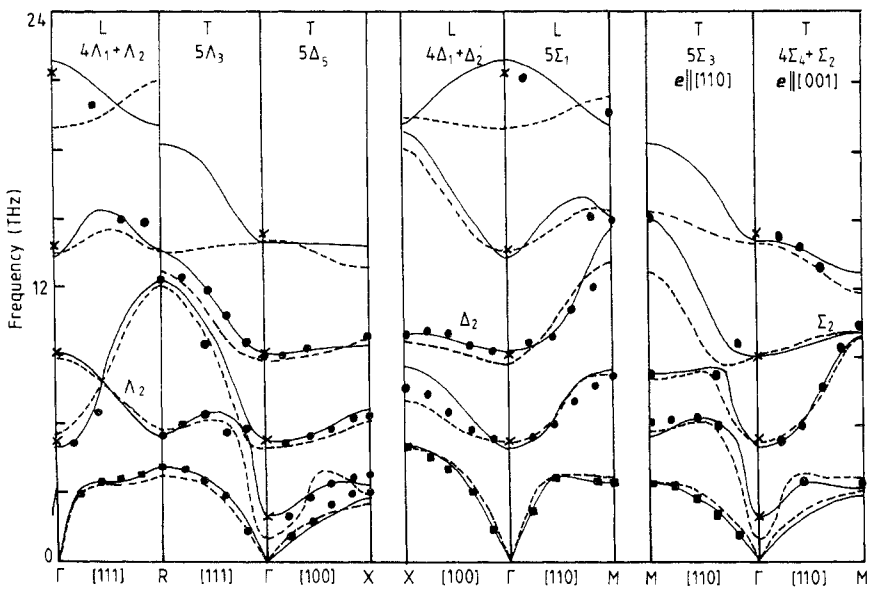

Figure 3. Phonon-dispersion curves calculated in $BaTiO_3$ at 421 K with model II (full curves) and compared with previous calculations of Jannot *et al* 1981 (broken curves).

branches TA and TO_1, particularly in the critical polarisation directions Δ_5 and Σ_4. Compared with $KTaO_3$ and $KNbO_3$, the TA dispersion surface in $BaTiO_3$ is less anisotropic as a function of mode polarisation. This is obvious when comparing the TA zone boundary energies for Σ_4 and Δ_5 with $e\|[001]$ versus Σ_3 ($e\|[1\bar{1}0]$), which appears at nearly the same frequencies (3 THz). This fact is well reproduced in our model and originates mainly from an important decrease (of about 30%) in the O–B chain parameters A_{OB} and B_{OB} and caused by a strong enhancement of the coupling parameters between the oxygen and baryum ions (more than 100% of the $KTaO_3$ value). Similar differences, but much less pronounced, are observed when making comparison with $SrTiO_3$.

In spite of the different fit of the starting conditions, the final values of the parameters of models I and II are comparable. This observation, together with the assumption of the same short-range interaction potentials within the TiO_6 octahedron in $BaTiO_3$ as for $SrTiO_3$, gives strong support to the numerical values obtained for the model parameters.

The shell charges Y_A, Y_B as well as Y_O are, in accordance with the shell-model theory, of negative sign. As shown in table 1, positive shell charges have been found for Sr in $SrTiO_3$ and for Ta (as strong as 7.83) in $KTaO_3$, which have also been applied to KTN by Kugel *et al* (1987). This sign can be interpreted in terms of overlap-charge polarisation (Bilz *et al* 1975). If the cation radius is significantly smaller than the O^{2-} one, the polarisation effects in the overlap region can be ascribed to the cation. K^+ and Ba^{2+}, both of nearly equal size and larger than Sr^{2+}, present negative shell charges. Although Ti^{+4} and Ta^{+5} have nearly the same size, and both are much smaller than the O^{2-} ion, a positive shell charge was obtained for Ta^{+5}, while a negative one results for Ti^{+4}.

The analysis of polarisability force constants, k, shows that Ba and Ti ions are rather rigid and that the main contribution of the electronic polarisability arises from the O^{2-} ions, as is usually observed in oxidic Perovskites. By neglecting the interference term in the calculations, the polarisabilities, α, of the oxygen ion can be estimated as shown in table 2, where comparison is made with the values taken in $KTaO_3$, $KNbO_3$ and $SrTiO_3$. The anisotropy of the oxygen polarisation will be discussed in § 3.3.

Table 2. Oxygen polarisability components in the O–A planes (α_{OA}) and along the O–B chains (α_{OB}) for $BaTiO_3$, $SrTiO_3$, $KTaO_3$ and $KNbO_3$.

	α_{OA} (Å^3)	α_{OB} (Å^3)
$BaTiO_3$	0.97	1.25
$SrTiO_3$	0.69	4.39
$KTaO_3$	0.93	2.44
$KNbO_3$	0.85	3.68

In figure 4 we show the one-phonon density of states corresponding to model II at 421 K. This is the frequency distribution calculated by the method of Gillat–Raubenheimer and weighted with the phonon thermal occupation number. On the various peak positions we indicate the phonons at symmetry points of the Brillouin zone which have nearly the same frequency. We include also for comparison the phonon density measured by Bouillot (1985) by time-of-flight neutron spectrometry at the ILL, Greno-

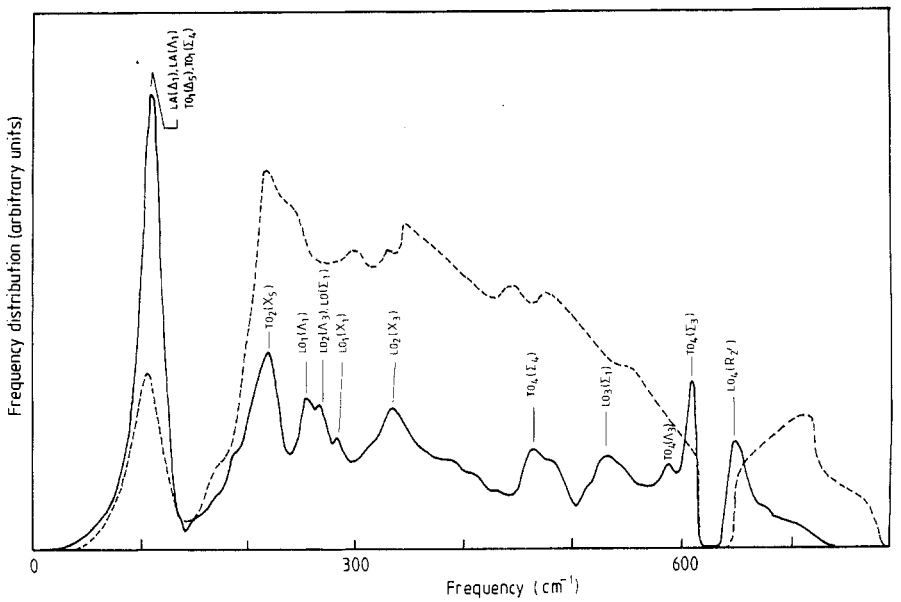

Figure 4. One-phonon density of states of $BaTiO_3$ calculated with model II (full curve) compared with the experimentally determined one (broken curve).

ble. It is seen that most of the observed features, also the gap between 625 and 640 cm^{-1}, are reproduced in the calculation.

3.2. *Self-consistent calculation of* $\langle w_{OB}^2 \rangle_T$, k_2^{O-B} *and* k_4^{O-B}

As shown by Luspin *et al* (1980), at $q = 0$ only the lowest frequency TO mode, $\omega(0, TO_1)$, depends on temperature. Since precisely the same effect is achieved by variation of the oxygen core–shell coupling $k_{OB}(T)$, we assume the remaining force constants of the model to be temperature independent, i.e. to neglect anharmonicities other than k_4^{O-B}. The limitations of such a treatment have already been remarked upon in §§ 1 and 2. The temperature dependence of $k_{OB}(T)$ is given by equations (3) and (4).

As a first step in the self-consistent evaluation of k_2^{O-B} and k_4^{O-B}, empirical values of $k_{OB}(T)$ as a function of temperature are determined for model II by adjusting the theoretical value $\omega(O, TO_1)$ to the infrared results (Luspin *et al* 1980). As shown in figure 5, in the temperature region between 600 and 1300 K, $k_{OB}(T)$ exhibits a linear behaviour, in agreement with equation 3 and 4 for $k_B T \ll \hbar\omega(q, j)$. At temperatures below 600 K, the stabilisation of the soft-mode frequency is reflected in a saturation of $k_{OB}(T)$.

With the initial values of $k_{OB}(T)$ determined so far, the thermal average of the oxygen shell displacement $\langle w_{OB}^2 \rangle_T$ can be calculated as function of temperature in (4). This implies the evaluation of $\omega(\boldsymbol{q}, j)$, $\boldsymbol{e}(\boldsymbol{q}, j)$ and $\boldsymbol{f}(\boldsymbol{q}, j)$ throughout the Brillouin zone for each T. In order to determine k_2^{O-B} and k_4^{O-B}, equation (3) is considered at the various temperatures where the previous calculations have been performed, thus yielding a system of linear equations from which k_2^{O-B} and k_4^{O-B} are obtained using a linear least-squares fit. $k_{OB}(T)$ can now be recalculated using (3) with $\langle w_{OB}^2 \rangle_T$ for the various chosen temperatures, and the whole calculation is repeated to achieve self-consistency.

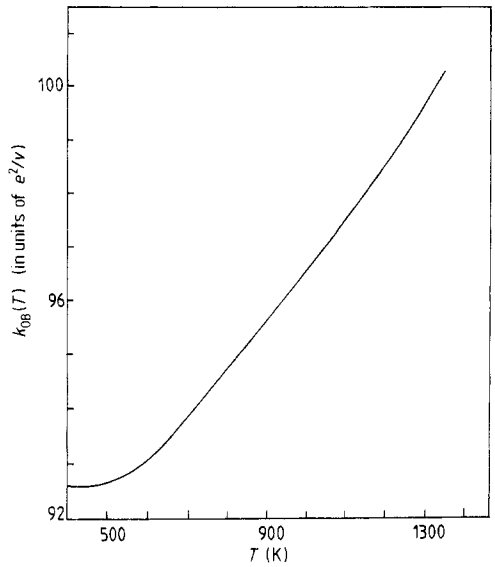

Figure 5. Temperature dependence of the oxygen core–shell coupling constant $k_{OB}(T)$ determined in $BaTiO_3$ using model II.

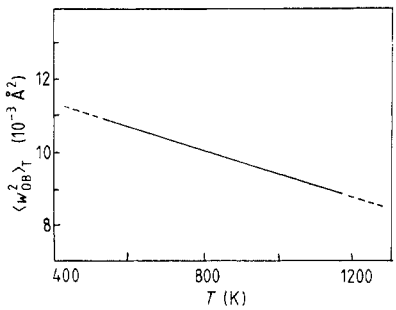

Figure 6. Temperature dependence of the thermal averaged oxygen shell displacement $\langle w_{OB}^2 \rangle_T$ calculated for $BaTiO_3$ with model II.

Figure 6 shows the temperature dependence of the oxygen-displacement thermal average $\langle w_{OB}^2 \rangle_T$ obtained. The first remarkable fact concerns the high values of $\langle w_{OB}^2 \rangle_T$ in $BaTiO_3$ (from 8 to 11 $\times 10^{-3}$ Å^2) compared with those obtained in $SrTiO_3$ (2 to 4 $\times 10^{-3}$ Å^2) by Migoni *et al* (1976) or in KTN (1 to 3 $\times 10^{-3}$ Å^2) by Kugel *et al* (1987). This very large amplitude of the oxygen shell displacements indicates a strong dynamical polarisation along the O–Ti chains. A second surprising feature is the unusual behaviour of $\langle w_{OB}^2 \rangle_T$ as function of temperature. Indeed, as seen in figure 6, $\langle w_{OB}^2 \rangle_T$ exhibits a slow linear decrease with increasing temperature, contradicting the coth law of equation 4, which normally leads to a quasi-linear enhancement with T, as observed in both $SrTiO_3$ (Migoni *et al* 1976) and the KTN system (Kugel *et al* 1987). So, the effect of the temperature factor is overwhelmed by an important decrease, with increasing temperature, of the shell amplitudes, in particular those of the low-frequency phonon modes. In other words, this means that when approaching the Curie temperature the oxygen-shell displacements show a highly critical divergence.

In the calculation of k_2^{O-B} and k_4^{O-B} values we discarded the temperatures in the vicinity of T_c where a stabilisation of $\omega(O, TO_1)$ and consequently of $k_{OB}(T)$ is observed and is connected to the cross-over from displacive to order–disorder behaviour (Müller *et al* 1982, Müller and Berlinger 1986). The values obtained for k_2^{O-B} and k_4^{O-B} are $137e^2/v$ and $-9000e^2/v$ Å^2 respectively. The negative sign of k_4^{O-B} is due to the decrease of $\langle w_{OB}^2 \rangle_T$ with increasing T. This is in contrast to the results obtained in $SrTiO_3$ and the KTN system, both of which show an increase in $\langle w_{OB}^2 \rangle_T$ with increasing T. However, Kugel *et al* observed in KTN that the rate of increase of $\langle w_{OB} \rangle_T^2$ as function of T decreases with increasing Nb concentration. This trend appears more drastically when switching from the displacive $SrTiO_3$ to the order–disorder-like $BaTiO_3$. Nevertheless, the occurrence of a negative k_4^{O-B} leads to a qualitatively different microscopic behaviour of $BaTiO_3$, since it implies a positive bare-harmonic frequency in the ferroelectric mode.

3.3. Temperature dependence of the phonons

Figure 7 represents the lowest frequency branches Λ_3, Δ_5 and Σ_4 as function of decreasing temperature. Only the TO_1 branch corresponding to the [100]-mode polarisation is affected by change of temperature and this with comparable variations from the centre to the border of the Brillouin zone. Unlike $SrTiO_3$, $KTaO_3$ and $KNbO_3$, the TA branch shows no modification with temperature. This is due to the fact that no crossing or exchange of eigenvectors between the TA and TO_1 branches occurs in $BaTiO_3$. The system keeps, even at temperatures near to T_c, a fairly isotropic TA dispersion.

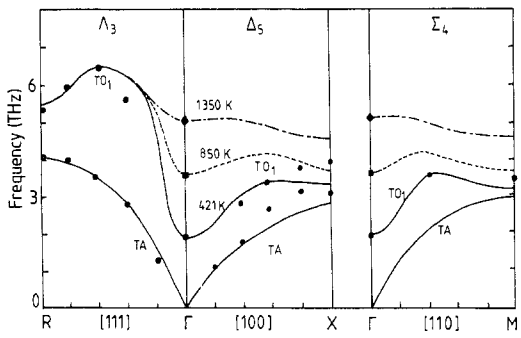

Figure 7. Low-frequency phonon dispersion curves calculated with model II of $BaTiO_3$ at several temperatures; 421 K, 850 K and 1350 K.

On the other hand, like in $KTaO_3$ the TO_1 dispersion surface in $BaTiO_3$ shows a strong anisotropy with respect to mode polarisation (parallel to the cube axis for modes Δ_5 and Σ_4 versus other polarisations for modes Σ_3 or Λ_3), while in $SrTiO_3$ the TO_1 dispersion is more isotropic. Nevertheless, the observed behaviour of the TA and TO_1 dispersion does not seem to be directly correlated with the anisotropy of the core–shell coupling at the oxygen. As shown in table 1 the ratio $k_{OA}/k_{OB}(T)$ is fairly large in $BaTiO_3$ and $SrTiO_3$ whereas it approaches unity in $KTaO_3$. Notice however that the anisotropy of the true electronic polarisability α is attenuated by the opposite influence of the short-range forces. The anisotropy of the oxygen polarisability, weaker in $BaTiO_3$ (model II) than in $SrTiO_3$, is in qualitative agreement with electron density distributions obtained by Weyrich and Siems (1986) through a self-consistent density functional approach.

4. Conclusions

The most relevant features pointed out in our calculations, namely the large negative quartic core–shell coupling at the oxygen and the unusual critical divergence of the oxygen shell eigenvectors, show even within our lattice dynamical point of view the strong anharmonic behaviour of $BaTiO_3$. Recent EPR measurements by Müller and Berlinger (1986) point to a strong local Ti anharmonicity and a tendency to ferroelectric order–disorder behaviour. The anharmonicity in Ti interaction does not contradict our model, since, as Migoni *et al* (1977) have shown, the adiabatic treatment of the local quartic electron–ion interaction at the O^{2-} ion leads to an effective quartic interaction for the Ti cores along the O–Ti chains. Also Kugel *et al* (1987) have observed in the KTN system that a strong enhancement of the core–shell O^{2-}-eigenvectors is connected with

a similar feature on the B ion. This picture is in further agreement with the finding of Weyrich and Siems (1985) that a pronounced flow of charge occurs from the O^{2-} towards the empty regions along the O–Ti chains when the ions are displaced according to the soft-mode eigenvector.

As already indicated in §§ 1 and 2, we are aware of the fact that our description of the lattice dynamics within the simple anisotropic oxygen polarisability model used here does not give an overall picture of the strong anharmonicity that exists in $BaTiO_3$. Since in particular the soft mode in $BaTiO_3$, as in $KNbO_3$, is particularly highly damped, third-order anharmonicity is required to explain the energy dependence of this mode. Thus our results which depend on ascribing this temperature dependence entirely to the particular quartic terms considered must be regarded as provisional.

Nevertheless, due to the stability and the low damping observed for the other phonon modes, we believe that the contribution which is analysed here and which has a selective influence on this TO_1 phonon mode, plays an important role on its softening mechanism.

The positive bare harmonic, soft-mode frequency and the negative quartic anharmonicity correspond to an effective potential for the soft-mode coordinate with a central minimum surrounded by finite barriers. If an additional positive sixth-order core–shell coupling at the oxygen is taken into account, such an effective potential acquires two secondary minima as proposed by Luspin *et al* (1981) in order to explain the relatively narrow crossover region between the displacive and the order–disorder regimes. Of course the dynamics in such a potential is not properly treated within the self-consistent phonon approximation, which projects only the oscillatory motion in the central minimum of the potential. It is even possible that the decrease of $\langle w_{OB}^2 \rangle_T$ with increasing T, and consequently the negative sign of k_4^{O-B} and the positive bare soft-mode frequency, arise as an artifact of the SPA. This may be the case if the temperature dependent frequency fitted to determine k_2^{O-B} and k_4^{O-B} represents actually a predominantly relaxational motion even at higher temperatures. This question, undoubtedly related to the origin of the overdamping, and the apparent crossover to an order–disorder behaviour near T_c, can be elucidated only through an exact numerical simulation of the dynamics. A preliminary exact analytical treatment of the one-dimensional version of our model (Bilz *et al* 1980, 1987) has been done by Dobry *et al* (1987) and further work is in progress.

References

Barker A S and Hopfield J J 1964 *Phys. Rev.* A **135** 1732
Bilz H, Benedek G and Bussmann-Holder A 1987 *Phys. Rev.* A **35** 4840
Bilz H, Buchanan M, Fischer K, Haberkorn R and Schröder U 1975 *Solid State Commun.* **16** 1023
Bilz H, Bussmann A, Benedek G, Büttner H and Strauch D 1980 *Ferroelectrics* **25** 339
Bouillot J 1985 private communication
Bruce A D and Cowley R A 1981 *Structural Phase Transitions* (London: Taylor and Francis)
Burns G and Dacol F H 1982 *Solid State Commun.* **42** 9
Cochran W 1960 *Adv. Phys.* **9** 387
Cowley R A 1964 *Phys. Rev.* **134** A981
Dobry A, Migoni R and Ceccatto H A 1987 private communication
Fleury P A and Worlock J M 1968 *Phys. Rev.* **174** 613
Fontana M D and Kugel G E 1985 *Japan. J. Appl. Phys.* **24** Suppl 2 223
Harada J, Axe J D and Shirane G 1971 *Phys. Rev.* B **4** 155
Inoue K and Asai N 1981 *J. Physique Coll.* **42** C6 430
Jannot B, Bouillot J and Escribe-Filippini C 1981 *Ferroelectrics* **37** 511
Kugel G E, Fontana M D and Kress W 1987 *Phys. Rev.* B **35** 813

Lines M E and Glass A M 1977 *Principles and Applications of Ferroelectrics and Related Materials* (Oxford: Clarendon)
Luspin Y, Servoin J L and Gervais F 1980 *J. Phys. C: Solid State Phys.* **13** 3761
Migoni R, Currat R, Perry C H, Buhay H, Stirling W G and Axe J D 1985 unpublished
Migoni R, Bilz H and Bäuerle D 1976 *Phys. Rev. Lett.* **37** 1158
Migoni R, Bilz H and Bäuerle D 1977 *Lattice Dynamics* ed. M Balkanski (Paris: Flammarion) p 650
Müller K A and Berlinger W 1986 *Phys. Rev.* B **34** 6130
Müller K A, Luspin Y, Servoin J L and Gervais F 1982 *J. Physique* **43** L537
Müller K A and Thomas H 1981 *Structural Phase Transitions (Springer Topics in Current Physics)* vol 23 (Berlin: Springer)
Presting H, Sanjurjo J A and Vogt H 1983 *Phys. Rev.* B **28** 6097
Shirane G and Hoshino S 1951 *J. Phys. Soc. Japan* **6** 265
Shirane G, Nathans R and Minkiewicz V J 1967 *Phys. Rev.* **157** 396
Spitzer W G, Miller R C, Kleinmann and Howarth L E 1962 *Phys. Rev.* **126** 1710
Stirling W G 1972 *J. Phys. C: Solid State Phys.* **5** 2711
Vogt H, Sanjurjo J A and Rossbroich G M 1982 *Phys. Rev.* B **26** 5904
Weyrich K H and Siems R 1985 *Z. Phys.* B **61** 63